Achievable rate approximation for massive MIMO with limited number of interfering clients

Telecommunication Systems manuscript No.
(will be inserted by the editor)

Achievable Rate Approximation for Massive MIMO with Limited Number of Interfering Clients

Omar Abu Ella · **Mohammed Elmusrati**

Abstract Massive MIMO has become a core technology for the next generation of wireless communications, and the non-linear group decoding schemes can achieve better spectral and energy efficiency, which in turn leads to higher data rates, especially with the assistance of non-orthogonal frequency multiple access (NOMA). The purpose of this paper is to study the problems of formulating performance of such systems. In particular, this paper, closely approximates the achievable rate of large-scale MIMO systems occupied by clients (users) using the optimal successive group decoding (OSGD) scheme to mitigate the co-channel interference. In addition, we produce a simple mathematical representation to accurately approximate the outage probability of this system. We also formulate the effective capacity of the considered system in a simple way. The results obtained by the Monte Carlo simulation show the validity of the derived formulas. The findings of this paper show that increasing the number of antennas linearly increases the expected value of the achievable rate and decreases its variance. In addition, the systems capacity is increasing in a logarithmic manner with the allocated power. Also, we notice that the distribution of the random achievable rate tends to be closely approximated with log-normal distribution as the number of antennas increases.

Keywords Achievable rate approximation · B5G/6G wireless technology · Massive MIMO · Successive group decoding · Non-orthogonal multiple access · Ergodic and effective capacity

O. Abu Ella
Department Electrical and Electronics Engineering, Misurata University, 2659 Eqzeer, Misurata, Libya
Tel.: +218-91-9770898
E-mail: omarabuella@eng.misuratau.edu.ly

M. Elmusrati
Faculty of Technology, University of Vaasa, Yliopistonranta 10, 65100, Vaasa, Finland.

1 Introduction

The rapid growth in demand for higher data rates, larger network capacity, better energy and spectral efficiency, and more mobility requirements for wireless communications are continued beyond 5G (B5G/6G) towards the 6G. All of the above requirements combined with the technical challenges imposed by scarcity of the frequency spectrum motivated the researchers to investigate new approaches to support the next generation networks to overcome the challenges facing wireless communication systems [1]. With this objective in mind, we recognized that one of the important strategies in this field is interference mitigation based technologies. This approach can be classified into two categories [2]: active techniques which are employed at the transmitter side [3–7], and passive techniques which are employed at the receiving side. In this context, the joint detection or the widely known as group decoding techniques are considered as passive interference mitigation schemes and they are intended for the interference cancellation at the receiver side. These techniques have drawn more attention [8–11] since they show an interesting performance improvement compared to the active counterparts, due to the overwhelming feedback overhead required for active schemes.

One of the recently introduced group decoding schemes is the optimal successive group decoding technique (OSGD) [12], where the receiver employs an interference-aware algorithm that intelligently determines (under the constraint of the receiver computational capability) the optimal ordered set of interfering users who should be jointly decoded with the desired signal and treats the other interfering signals as noise [13].

1.1 Related Work

This sub-section is dedicated to present the progress in the research efforts which eventually leaded to the performance characterization of the massive MIMO and successive grope decoding schemes as summarized in Table 1. It is well known that the problem of evaluating the performance of multiple antenna systems is not new topic in the wireless communication literature. For instance, the work of Telatar [14] has laid the basis of the formulation of MIMO system capacity, where he has derived an exact expression for the mean of multi-antenna system capacity under the assumption of using Gaussian channels. Then, Rapajic and Popescu [15] have derived a closed-form expression for the information capacity of the random MIMO channel signature. Also, in [16] the authors calmed that the capacity of MIMO system converges in distribution to a Gaussian random variable, and gave closed-form formulas for its mean and variance. They have characterized the asymptotic probability distribution of the capacity of a multiple-antenna in the Rayleigh-fading channel as the numbers of transmit and receive antennas become large. The problem of these mentioned research work that they have not considered the practical transmit/ receive schemes.

This matter has been addressed in [17] which computed capacity of large MIMO system that uses an MMSE precoder based on asymptotic analysis. However, the authors of this paper did not take co-channel interference into account. In contrast, [18] presented asymptotic capacity analysis of block diagonalisation precoding with space-time block code schemes which eliminates inter-user interference for wireless communication systems. Also, [19] provided an explicit expression of the massive MIMO user capacity in the pilot-contaminated regime where the number of users is larger than the pilot sequence length. Furthermore, [20] established formulation of the achievable sum-rate of massive MIMO wireless backhaul links in heterogeneous cellular networks, which employ simple maximum ratio combining receive filter and maximum ratio transmission precoding to mitigate interference. Nevertheless, it is still a fact that all the derived formulae in the above stated research papers are influenced by the utilization of linear precoding or linear post-processing schemes.

However, from another point of view, the literature includes a wide range of research focusing on the analysis of the capacity of non-linear interference cancellation decoders, which are mostly deployed at the receiving side. For instance, Authors of [21] analyzed the transmission capacity of wireless Ad Hoc networks with successive interference cancellation. Also, [22] characterized the Transmission Capacity Region (TCR) in D2D integrated cellular networks when two prevalent interference management techniques: power control, and successive interference cancellation are utilized. In [23] the authors aimed to evaluate the performance of the MIMO-NOMA system which uses SIC, their research added to the formulation of outage probability, and channel capacity of such system. While [24] focused on comparative performance analysis among hybrid NOMA schemes such as MIMO-NOMA, NOMA with generalized space shift keying (NOMA-GSSK), and STBC-Aided Cooperative NOMA (STBC-CNOMA) in terms of spectral efficiency (SE) and the number of SIC occurrence. In [25] the researchers investigated the performance of integrated satellite-terrestrial networks (ISTNs) based on NOMA with relay selection and imperfect SIC and derived closed-form expressions for the outage probability and ergodic capacity of the considered networks. Moreover, the anthers of [26] studied the achievable sum-rate of the two-user Gaussian interference channel when joint decoding is replaced by successive decoding.

The problem of the majority of the above-mentioned research work is that they only considered the characterization of the iterative MIMO system based on employing conventional sub-optimal interference cancellation schemes. Where the users at the receiving side independently decode and cancel out each undesired user from the receiving signal (one by one), and they do not rely on the joint decoding which is the optimal strategy. Therefore, other researchers focused on analyzing the capacity of the joint decoding schemes such as: The authors of [27] presented the inner and outer capacity boundaries for joint decoding and independent decoding, along with physical explanations as to how these boundaries can be achieved. In addition, [28] investigated the ergodic capacity of the return link of a multibeam satellite system, where user signals are jointly decoded to cancel self-interference. Also, in [29] where the authors obtained an approximation for the rate region of the many-to-one and one-to-many Gaussian interference channels within a constant number of bits. In [30] the authors characterized the spectral efficiency of massive MIMO when the BSs are allowed to jointly decode the received signals, for both finite and asymptotic number of antennas.

From the definition of successive interference cancellation as decoding and eliminating strong interfering signals independently until the wanted signal can be decoded, and by referring to the more complicated simultaneous decoding of all the signals as joint decoding, we can define successive group decoding (SGD) as the scheme of jointly decoding and eliminating subgroups (partitions) of interfering signals successively until the wanted signal is decoded. Therefore, based on its working strategy and with the capability of determining the optimal size of the jointly decoded subgroup of signals in each decoding stage, the optimal SGD can satisfy the trade-off between the complexity that the system can sustain and the required performance to maintain the desired QoS level. Subsequently, characterizing the performance of

Table 1 Previous work

Topic	Aspects and References
Capacity analysis of MIMO systems employing only linear precoding or linear post-processing schemes.	Basis of MIMO system capacity [14] Closed-form of random MIMO Signature [15] PDF of MIMO capacity approximated with normal distribution [16] Analyzed the capacity of Large MIMO with MMSE [17] Presented the asymptotic capacity analysis BDP with STBC [18] Massive MIMO capacity [19] achievable sum-rate of massive MIMO wireless backhaul, using (MRC) [20].
Capacity analysis for the nonlinear successive interference cancellation. Where the users at the receiving side independently decode and cancel out each undesired user from the receiving signal (one by one), and they do not rely on the joint decoding which is the optimal strategy.	Analysis of transmission capacity of wireless Ad Hoc networks with successive interference cancellation [21] Characterizing the transmission capacity region (TCR) in D2D integrated cellular networks [22] Evaluate the performance of the MIMO-NOMA system with SIC [23] Comparative performance analysis of SIC among hybrid NOMA schemes such as, NOMA-GSSK and STBC-CNOMA [24] Investigating the performance of integrated satellite-terrestrial networks (ISTNs) based on NOMA with relay selection and imperfect SIC [25] Studying the achievable sum-rate of the two-user Gaussian interference channel when joint decoding is replaced by successive decoding [26].
Capacity analysis of the joint decoding (simultaneous decoding of all the signals).	Analysis of the inner and outer capacity boundaries for joint decoding and independent decoding [27] Investigating the ergodic capacity of the return link of a multibeam satellite system, where user signals are jointly decoded to cancel self-interference [28] Obtaining an approximation for the rate region of the many-to-one and one-to-many Gaussian interference channels within a constant number of bits [29] Characterizing the spectral efficiency of massive MIMO when the BSs are allowed to jointly decode the received signals, for both finite and asymptotic number of antennas [30].
Capacity analysis of successive group decoding, i.e., jointly decoding and eliminating subgroups (partition) of interfering signals successively until the wanted signal is decoded.	Preliminary results of approximating the achievable rate of SGD for massive MIMO system [31].

the SGD is an important task to understand the limits of the scheme which fills the gap between the SIC and JD systems.

1.2 Paper Objectives

Motivated by the lack of the performance analysis of the successive group decoding techniques and because of its potential to achieve higher data rates in the interfering environments [32]. Also since massive MIMO, non-orthogonal multiple access (NOMA) [33, 34] and small cell [35–39] are promising key technologies for beyond 5G (B5G/6G) of wireless communications [1]. We aim in this paper to mathematically evaluate the performance of SGD schemes by considering the problem of formulating the achievable rate, outage and effective capacities the 3-client (nodes) utilizing OSGD to mitigate interference in massive MIMO system.

The considered scenarios in this paper can be encountered in massive MIMO small cell backhauling system, or in massive MIMO system utilizes non-orthogonal multiple access (mMIMO-NOMA) to increase the number of the simultaneous active users. The produced mathematical expressions can consequently facilitate determining the QoS level of such systems. Our objectives eventually will go in the stream of shading some light on the performance limits of the next generations of wireless communication systems.

1.3 Paper Contributions

To this end and to the best of author's knowledge, there is no known research work that has computed the exact or the approximate achievable rate of the nonlinear optimal successive group decoder for a massive MIMO system, except for our brief results presented in earlier conference paper [31]. Even though the results of the mentioned paper look at first glance to be similar to the outcomes of this article, yet it is still a fact that we have made major modifications in all computations and the analysis to produce the new results reported here.

– In contrast to the work in [31] we have changed the fundamental hypothesis in the computations. For instance,

Table 2 Paper structure

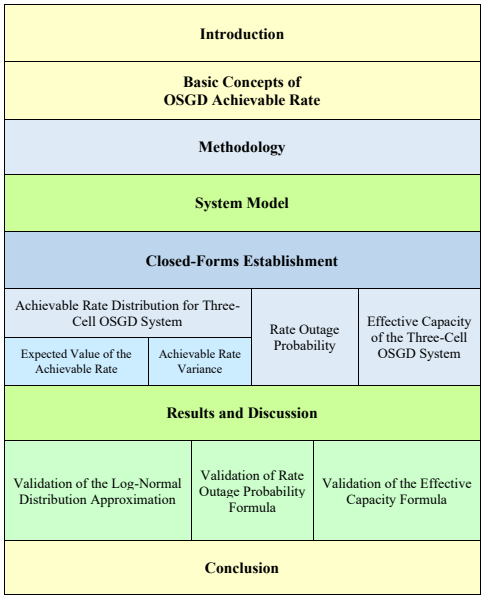

we previously assumed that the randomness of the achievable rate could be tightly characterized using the normal distribution. However, we found through this work that it is much suitable to approximate it with a log-normal distribution.

– In addition, it is worth mentioning that in the previous conference paper, we did not investigate an important metric which characterizes the quality of experience (QoE) in the system, i.e., the QoS from the end-user point of view. This metric is known as the effective capacity, and it will be discussed in detail in this article.

The remainder of this paper is organized as presented in Table 2: Section 4 describes the system model considered in this paper. Section 2 briefly reviews the concepts of the OSGD achievable rate. Section 5 discusses the formulation of achievable rate, addresses the formulation of rate outage expression. Subsequently, it extends the argument to include the effective capacity conception for the system of interest. After presenting the validation of the proposed formulas via the numerical results in Section 6, we summarized our conclusions in Section 7.

2 Basic Concepts of OSGD Achievable Rate

This section is dedicated to outline the fundamentals of analytical computations of the OSGD. Detailed discussion of the OSGD optimality and its employed algorithms are not in the scope of this paper and can be found in [12]. However, for the sake of the readers' convenience, we briefly reproduced the main concepts related to the OSGD system achievable rate. So, assuming that for any two arbitrary disjoint sets $\mathscr{U},\mathscr{V}\subseteq\mathscr{M}$, where $\mathscr{M}$ is the set of integer indices of all active users in the system, the receiver of interest is d. Then, the desired source will be transmitter d, and given all user's rates $\boldsymbol{R}=[R_j]_{j\in\mathscr{M}}$, the instantaneous achievable rate region $\mathscr{C}_d(\mathscr{U},\mathscr{V})$ can be described as [12]

$$\mathscr{C}_d(\mathscr{U},\mathscr{V})=\left\{\boldsymbol{R}\in\mathbb{R}_+^{|\mathscr{U}|}:\sum_{j\in\mathscr{D}}R_j\leq\boldsymbol{\mathcal{R}}_d(\mathscr{D},\mathscr{V}),\forall\mathscr{D}\subseteq\mathscr{U}\right\} \tag{1}$$

$$\boldsymbol{\mathcal{R}}_d(\mathscr{D},\mathscr{V})\leq\log\left|I+\tilde{\mathbf{H}}_{\mathscr{D}}^{(d)\mathscr{H}}\left(I+\tilde{\mathbf{H}}_{\mathscr{V}}^{(d)}\tilde{\mathbf{H}}_{\mathscr{V}}^{(d)\mathscr{H}}\right)^{-1}\tilde{\mathbf{H}}_{\mathscr{D}}^{(d)}\right|, \tag{2}$$

where the channel realization

$$\tilde{\mathbf{H}}^{(d)}=\left[\sqrt{P}\mathbf{H}_d^{(d)},\sqrt{\alpha_1 P}\mathbf{H}_1^{(d)},\sqrt{\alpha_2 P}\mathbf{H}_2^{(d)}\right]. \tag{3}$$

where, $\mathbf{H}_d^{(d)}$ is the fading channel matrix between the receiver of interest and its intended (desired) transmitter. $\mathbf{H}_1^{(d)}$ and $\mathbf{H}_1^{(d)}$ are the fading channel matrices between the receiver of interest and its first and second interfering transmitter respectively.

Considering the valid partition of $\mathscr{M}$ for the user of interest d: $\underline{\mathscr{Q}}^d=\mathscr{Q}_1^d,\ldots,\mathscr{Q}_{p_d}^d,\mathscr{Q}_{p_d+1}^d$, we can assume that all users of this partition can be decoded by the desired receiver only if

$$\boldsymbol{R}_{\mathscr{Q}_m^d}\in\mathscr{C}_d(\mathscr{Q}_m^d,\cup_{j=m+1}^{p_d+1}\mathscr{Q}_j^d),\quad\forall m\in\{1,\ldots,p_d\}, \tag{4}$$

where, $\boldsymbol{R}_{\mathscr{Q}_m^d}$ is the decodable rate vector for receiver d before the increment. For the valid partition $\underline{\mathscr{Q}}^d$ of the receiver d we define $\mathbf{r}_{\mathscr{Q}_m^d}^d=[r_j^d]_{j\in\mathscr{Q}_m^d}$. Then, the fair rate increment which guarantee that all users in $\{\mathscr{Q}_1^d,\ldots,\mathscr{Q}_{p_d}^d\}$ are decodable at the receiver d is defined by

$$r_d(\underline{\mathscr{Q}}^d)\triangleq\max r_j^d,\quad\forall j\in\mathscr{M}, \tag{5}$$

where, r_j^d is the tolerable rate increment of user j at the receiver of interest d.

such that

$$\widetilde{\boldsymbol{R}}_{\mathscr{Q}_m^d}=\boldsymbol{R}_{\mathscr{Q}_m^d}+\mathbf{r}_{\mathscr{Q}_m^d}^d\in\mathscr{C}_d(\mathscr{Q}_m^d,\cup_{j=m+1}^{p_d+1}\mathscr{Q}_j^d),\quad\forall m\in\{1,\ldots,p_d\}, \tag{6}$$

Under the fairness (equal rate increment) constraint, and assuming that $\widetilde{\boldsymbol{\mathcal{Q}}}^d$ ensembles all the valid partitions $\underline{\mathscr{Q}}^d$, then, at the receiver d the maximum user rate increment is given by

$$r_{\underline{\mathscr{Q}}^d}^*\triangleq\max_{\underline{\mathscr{Q}}^d\in\widetilde{\boldsymbol{\mathcal{Q}}}^d}r_d(\underline{\mathscr{Q}}^d). \tag{7}$$

We can notice that solving (7) using the exhaustive search considering all combinations of $\underline{\mathscr{Q}}^j$ is complex, especially for large number of users. However, by defining the following rate margin metric

$$\triangle_d(\mathscr{D},\mathscr{V}) \triangleq \boldsymbol{\mathcal{R}}_d(\mathscr{D},\mathscr{V}) - \sum_{j\in\mathscr{D}} R_j, \tag{8}$$

and using the properly designed algorithm proposed in [40], we can find the optimal ordered partition $\underline{\mathscr{Q}}^{d*}$ which minimizes the rate margin $\triangle_d(\mathscr{D},\mathscr{V})$, or equivalently maximizes the rate increment r_d, i.e.,

$$\begin{aligned}\underline{\mathscr{Q}}^{d*} &= \arg\max_{\underline{\mathscr{Q}}^d\in\widetilde{\boldsymbol{\mathcal{Q}}}^d} r_d(\underline{\mathscr{Q}}^d)\\ &= \arg\min \triangle_d(\mathscr{D},\mathscr{V}).\end{aligned} \tag{9}$$

Therefore, the maximum achievable rate (capacity) of OSGD can be given by

$$\widetilde{\boldsymbol{R}}_{Q_m^d} = \boldsymbol{R}_{Q_m^d} + \mathbf{r}^*_{Q_m^{d*}}. \tag{10}$$

3 Methodology

Due to the nonlinear characteristics of the successive group decoding schemes combined with the high processing complexity of the large number of antennas in massive MIMO systems, all of that makes the derivation of an analytical expressions for the performance characteristics of such systems a highly intractable mathematical challenge. However, motivated by the essential importance of the optimal successive group decoding technique to achieve higher data rates and to move a step forward towards better understanding of such schemes, we have considered the problem of formulating the achievable rate for the three-cell system that deploys massive MIMO and nonlinear OSGD receivers.

In this article, to avoid being trapped into the prohibitively complicated mathematical computations associated with the optimal joint interference decoding processes, we chose to work on this problem differently using a semi-analytical approach. So, we approach this problem through finding the best fitted mathematical functions for the numerically generated data via Monte-Carlo simulation. This eases the task of extracting good approximation for the distribution of the achievable rate in the system as a function of SNR and number of antennas. Then we used this approximations to obtain highly accurate formulas which give initial guidelines for more general prospective analysis. In fact the used method in this work could be used in future studies to investigate further topics in this area of research, including studying the effect of: spatial channels correlation, unequal power allocation, and the number of interferers on the overall massive MIMO system performance, especially for those systems which deploy receive-side interference cancellation schemes.

We accomplished our objectives of characterizing the OSGD system performance through exploring the empirically generated functions employing the statistical analysis of large data set collected from the numerical results of the modeled system described in Section 4. To evaluate the performance of several considered scenarios in this paper, we have designed various Monte-Carlo simulation setups, which generated millions of outcome samples through hundreds or thousands of channel realizations for each massive MIMO configuration. These scenarios have been implemented according to different parameters, such as, SNR level, number of antennas, the target transmission rate and the required QoS level which represented through the buffering constraints.

4 System Model

Despite the fact that in massive MIMO, increasing the number of served users helps to increase the spatial multiplexing gain of the large-scale MIMO system by exploiting the spatial diversity because of the terminal users being located apart [41]; yet we mainly have interested in this paper in the investigation and characterizing the performance of massive MIMO system when only few numbers of interfering (nodes/clients) are actively coexisted. Examples of reasonable scenarios of such schemes in practice include: the communication between macro BS and its associated micro cell BSs or in more generalized setup as the non-line-of-sight small cell wireless backhaul system [42–45].

Therefore, through the remainder of this paper, we only consider the system layout of the interfering clients who are sharing the same resources in the three-cell system as depicted in Fig. 1. For the sake of discussion simplicity and without loss of generality, they might be considered to be three macro-cell BSs communicating through broadcasting channel with their associate small-cell or micro-cell BSs. Again, it is worth mentioning that although the real communication system is often occupied with much larger number of nodes, we take into account only the effect of few clients, who are physically and simultaneously sharing the same resources and they are not distinguishable in time, frequency nor space and they have non-ignored interfering impact on the communication link of each other. From an other point of view, as referred in [2] according to field measurement study conducted by the Universal Mobile Telecommunications System Network, it is reported that even at much simpler communication system which consists only of BS and orthogonal users, the simultaneous active number of interfering users is very small in the communication system.

In the considered scenario, we assume that the receiver of interest is (Client-1) in the downlink case. Or it can be (Macro-BS-1) in the uplink case. In both cases this receiver

is assumed to have the capability employing the optimal successive group decoding (OSGD) technique to mitigate co-channel interference coming from the two interfering sources which are (BS_2 and BS_3) in the downlink scenario or (Client-2 and Client-3) in the uplink case.

We consider the temporally uncorrelated discrete model of a slow-fading channel, and we assume that both base station of interest and its designated client are equipped with large number (tens) of antennas N. The utilization of massive MIMO over wide range of frequency bands and use-case differences of massive MIMO in millimeter wave and in sub-6 GHz bands are addressed with great physical details in [46–48], which examined the feasibility and suitability of massive MIMO in different propagation scenarios. And it concluded that massive MIMO can be used for Backhaul/fronthaul links in both millimeter-wave bands or in bands below 6 GHz by multiplexing many LoS or even in NLoS links. Also [49] clearly reported that by comparing the performance of a practical UMa scenario at 3.5 GHz to the i.i.d. channel, the ratios of above 70% are achieved when the number of antenna array elements are increased.

We assume that each base station and its intended client communicate with each other, but due to the broadcasting nature of wireless channel the transmitted signal is received by other unintended clients. In addition, we assume that the receiver of interest is only interested in the signal transmitted by its own designated transmitter; however, it is aware of the coding scheme employed by the other two transmitters and may choose to decode one or both of them only if it presumes doing that will assist the decoding of its intended signal. Therefore, the received signal of this receiver at the nth symbol interval through this interference environment can be expressed by

$$\mathbf{y}[n] = \sqrt{P}\mathbf{H}_d\mathbf{x}_d[n] + \sqrt{\alpha_i P}\sum_{i=1}^{2}\mathbf{H}_i\mathbf{x}_i[n] + \mathbf{z}[n], \tag{11}$$

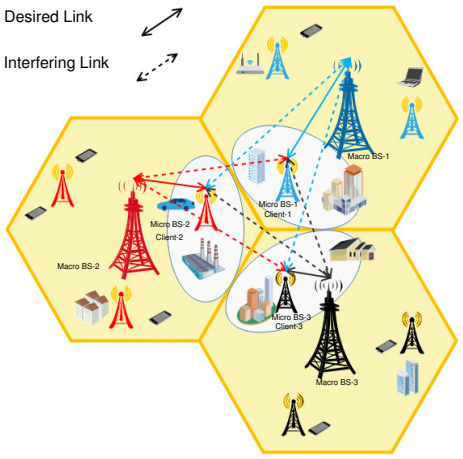

Fig. 1 System Layout.

where $\mathbf{y}[n]$ is the $N \times 1$ received signal vector. In this system we assume a quasi static Rayleigh fading scenario, i.e., the fading seen by the receiver of interest from its intended transmitter denoted by $\mathbf{H}_d$ and from the interfering senders denoted by $\mathbf{H}_i$ have a Rayleigh distribution, where the elements of those channels are generated as normalized independent and identically distributed (i.i.d.) complex Gaussian random variables with zero mean and unit variance.

In this paper, $\mathbf{H}_d$ is presumed to be perfectly known to the receiver of interest, but it is not known to any of the transmitters. $\mathbf{z}[n]$ is the $N \times 1$ represents the complex AWGN vector at the receiver, it is assumed to typically have i.i.d. $\sim \mathscr{CN}(0,1)$ elements and it is temporally uncorrelated. P indicates the average transmitted power. α_i stands for the cross-talk factor from the undesired transmitters, i.e., it adequately represents the relative propagation path loss of the interference channel. Finally, $\mathbf{x}_d[n]$ and $\mathbf{x}_i[n]$ represents a unit power symbol vector transmitted from the desired and interfering user respectively during the nth specific time interval.

Here, we would highlight that the setup was built basically on the assumption of temporally uncorrelated discrete model of slow flat fading environment to represent the broadcasting interference channel. According to [50] the feasibility of the assumption of i.i.d. Rayleigh fading channel model for the theoretical analysis of massive MIMO system is widely adopted. This assumption relies on the fact that the correlation and mutual coupling between transmit antennas or receiver antennas can be ignored if the array elements are properly spaced. The co-channel interference level between the three neighboring cells was controlled by adjusting a cross-talk factor. Hence, we could extract a reasonable approximation for the distribution of the achievable rate as a function of the two fundamental design parameters which are: SNR and the number of antennas. All considered ranges and values of the simulation parameters are clearly stated in the Section 6 or depicted on the figures.

5 Closed-Forms Establishment

As depicted in Fig. 2, this section addresses the formulation of achievable rate, rate-outage expressions, and it also extends the argument to include the derivation of effective capacity for the system of interest.

5.1 Achievable Rate Distribution for Three-Cell OSGD System

Through the statistical analysis of the achievable rate of the three-cell system equipped with massive MIMO and OSGD, we noticed that the statistical distribution of the data significantly fits the log-normal. Therefore, we started seeking an

efficient way to estimate the parameters of this distribution. A simple and effective way to accomplish this task is the 2-D surface fitting method. So, we constructed, tested and modified our model to attain the best formula, i.e., the most accurate in terms of the mean square error (MSE). As we previously said, based the collected set of data generated by the Monte-Carlo simulation, we assumed that the randomness of achievable rate is precisely characterized by the log-normal distribution. This hypothesis could also be deduced as follows,

Given that the ergodic capacity of any fading channel can be expressed as in [51]

$$C = \int_{\gamma} log(1+\gamma)p(\gamma)d\gamma \tag{12}$$

where, $p(\gamma)$ denotes the probability density function (pdf) of the fading process. Also, since the distribution of the local average power of the wireless systems in both terrestrial and satellite channels at indoor or outdoor for long and short-term is widely accepted to be log-normal [52–56]. And relaying on fact stated in [57–59] that the sum and the product of log-normal random variable is well approximated by another log-normal variable. Therefore, we can safely assume that achievable rate is well approximated with log-normal distribution. The validation of this assumption will presented later in this paper in subsection 6.1 and it is confirmed through the high consistency between the histogram of the numerical values of the achievable rate obtained via Monte-Carlo simulation and the log-normal probability density function (PDF). Moreover, it is important to keep in mind that achievable rate is always greater than or equals zero. This consequently makes the assumption of log-normal distribution (which is one-sided distribution) more appropriate to characterize the achievable rate of the system comparing with the (two-sided) normal distribution. Therefore, we assume that the distribution of the capacity of the three-cell massive MIMO OSGD system described in section 4 can be tightly approximated by the log-normal distribution with mean ($\hat{m}_c$) and variance ($\hat{v}_c$), i.e.,

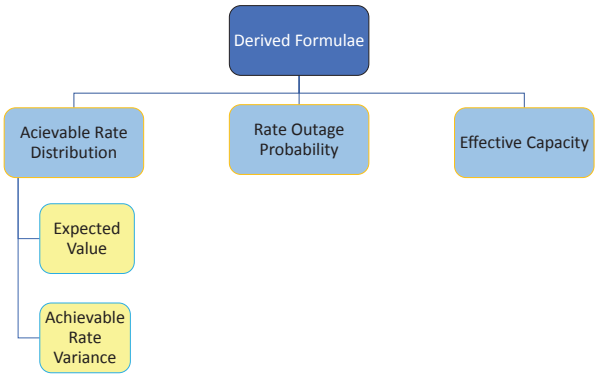

Fig. 2 Derived Formulae.

$$C \sim \mathscr{LN}(m_c, v_c), \tag{13}$$

or equivalently

$$\ln(C) \sim \mathscr{N}(\mu_c, \sigma_c^2), \tag{14}$$

where, μ_c and σ_c^2 denote the mean and variance of the corresponding normal distribution respectively, hence, we can express them in terms of m_c an v_c as follows,

$$\mu_c = \ln\left(\frac{m_c^2}{\sqrt{m_c^2+v_c}}\right) \tag{15}$$

and

$$\sigma_c = \sqrt{\ln(1+\frac{v_c}{m_c^2})} \tag{16}$$

To compute the best estimate for the log-normal distribution parameters, we used the least squares (LS) method. The basic idea of this approach is to minimize the sum of the squared error of the estimated values.

$$\sum_i \mathscr{E}_i^2 = \sum_i \left(\mathscr{S}_i - \hat{\mathscr{S}}_i\right)^2 \tag{17}$$

where $\mathscr{S}_i$ and $\hat{\mathscr{S}}_i$ are the exact and the estimated sample value respectively.

In the following subsections we describe and compute the parameters of the proposed models to determine the achievable rate mean (ergodic capacity) and variance of the three-cell massive MIMO system with OSGD capability.

5.1.1 Expected Value of the Achievable Rate

Achievable rate expected value m_c or the ergodic capacity of the desired user that uses OSGD scheme depends on system SNR level γ and the number of deployed antennas N. Using the aforementioned set of simulation data, we recognized that the expected value of the system achievable rate can be modeled tightly at high confidence level $> 95\%$ as follows:

$$\hat{m}_c(\gamma,N) = a_m \log_2\left(1+\left[2\left(\frac{1}{N}\right)^{b_m}+c_m\right]\gamma\right)N \tag{18}$$

where, a_m, b_m and c_m are constants.
The above model can be simplified to the following form

$$\hat{m}_c(\gamma,N) = Na_m \log_2(1+B_m\gamma) \tag{19}$$

where

$$B_m = \left[2\left(\frac{1}{N}\right)^{b_m}+c_m\right] \tag{20}$$

We promptly see that OSGD scheme achievable rate can be equivalently viewed as the achievable rate of Na_m independent sub-channels with weighted SNR. The gap of the achievable rate comparing with achievable rate of full N-channel system is due to the non-orthogonality between those sub-channels, and the additional SNR loss because of the residual interference which treated as white noise instead of canceling it in case of receiving relatively low interference power. Therefore, for K-interfering users system with large N, it is reasonable to expect B_m to be less than K.

Now, we can compute coefficients, a_m, b_m and c_m via the Least Squares (LS) algorithm as follows:

$$\{a_m, b_m, c_m\}^{opt} = \arg \min_{a_m, b_m, c_m \in \Re} \sum_i \mathscr{E}_i^2(\hat{m}_c) \tag{21}$$

where, the error of the estimated mean using the ith observation is given by

$$\begin{aligned}\mathscr{E}_i(\hat{m}_c) &= m_c(i) - \hat{m}_c \\ &= m_c(i) - a_m \log_2\left(1 + \left[2\left(\frac{1}{N_i}\right)^{b_m} + c_m\right]\gamma_i\right) N_i \end{aligned} \tag{22}$$

$$\begin{aligned}&\sum_i \mathscr{E}_i^2(\hat{m}_c) = \\ &\sum_i \left\{ m_c(i) - a_m \log_2\left(1 + \left[2\left(\frac{1}{N_i}\right)^{b_m} + c_m\right]\gamma_i\right) N_i \right\}^2 \end{aligned} \tag{23}$$

To find the values of the model coefficients a, b, and c correspond to the minimum of the multivariate error function; we compute the partial derivative of (23) with respect to each coefficient and force it to zero,

$$\frac{\partial \sum_i \mathscr{E}_i^2(\hat{m}_c)}{\partial a_m} = 0, \frac{\partial \sum_i \mathscr{E}_i^2(\hat{m}_c)}{\partial b_m} = 0, \frac{\partial \sum_i \mathscr{E}_i^2(\hat{m}_c)}{\partial c_m} = 0, \tag{24}$$

equivalently we have,

$$\begin{aligned}&\frac{\partial \sum_i \left(m_c(i) - a_m \log_2\left(1 + \left[2\left(\frac{1}{N_i}\right)^{b_m} + c_m\right]\gamma_i\right) N_i \right)^2}{\partial a_m} = 0 \\ &\frac{\partial \sum_i \left(m_c(i) - a_m \log_2\left(1 + \left[2\left(\frac{1}{N_i}\right)^{b_m} + c_m\right]\gamma_i\right) N_i \right)^2}{\partial b_m} = 0 \\ &\frac{\partial \sum_i \left(m_c(i) - a_m \log_2\left(1 + \left[2\left(\frac{1}{N_i}\right)^{b_m} + c_m\right]\gamma_i\right) N_i \right)^2}{\partial c_m} = 0 \end{aligned} \tag{25}$$

Then, by solving the system of equations in (25) according to the large set of collected data we have:

$$a_m = \frac{1}{3}, b_m = 3$$

and

$$c_m = 3 + 2\log(3) - \frac{2}{\log(2)} + \frac{1}{\log(1+\gamma)+3}.$$

Therefore, (18) could be simplified to be as follow

$$\begin{aligned}&\hat{m}_c(\gamma, N) = \\ &\frac{N}{3}\log_2\left[1 + \gamma\left(\frac{2}{N^3} + 3 + 2\log(3) - \frac{2}{\log(2)} + \frac{1}{\log(\gamma+1)+3}\right)\right] \end{aligned} \tag{26}$$

5.1.2 Achievable Rate Variance

In this part we aim to model the variance of the achievable rate v_c. Considering the statistics of the collected data, we noticed that the variance of the system achievable rate grows with SNR as a result of the rise of the achievable rate itself with SNR. This increase follows an upper bounded logistic function. From an other point of view, and as expected, through carefully analysis of the statistics of the collected data; we observed that increasing the number of employed antennas slightly decreases the variance of the system achievable rate. This reduction is tightly following a curve of power function. This behavior is expected, because the number of employed antennas N is a critical affecting factor on the scheme achievable rate. In other words, the system achievable rate is strongly and positively correlated with the system size. Hence, in consonance with the law of large number, we expect that increasing the size of this dimension should decrease the fluctuations (i.e., the variance) of any correlated function.

Therefore, we chose to express the variance using the following model:

$$\hat{v}_c(\gamma, N) = \frac{a_v}{1 + \phi e^{-b_v \gamma_{dB}}} \tag{27}$$

where $\gamma_{dB} = 10\log_{10}(\gamma)$, $\phi = \alpha_v N^{\beta_v} + \chi_v$
Then, using the similar steps of the procedure in 5.1.1, we compute the coefficients, a_v, b_v, α_v, β and χ_v through the (LS) algorithm as follows:

$$\{a_v, b_v, \alpha_i, \beta_v, \chi_v\}^{opt} = \arg \min_{a_v, b_v, \alpha_v, \beta_v, \chi_v \in \Re} \sum_i \mathscr{E}_i^2(\hat{v}_c), \tag{28}$$

where

$$\begin{aligned}\mathscr{E}_i(\hat{v}_c) &= v_c(i) - \hat{v}_c \\ &= v_c(i) - \left(\frac{a_v}{1 + \phi_i e^{-b_v \gamma_{dBi}}}\right) \end{aligned} \tag{29}$$

and,

$$\sum_i \mathscr{E}_i^2(\hat{v}_c) = \sum_i \left(v_c(i) - \left(\frac{a_v}{1 + \phi_i e^{-b_v \gamma_{dBi}}}\right)\right)^2 \tag{30}$$

To obtain the values of the model coefficients (a_v, b_v, α_v, β_v, and χ_v) which satisfy the objective function in (28), we compute the partial derivative of both sides of (30) with respect to each coefficient and equate the result to zero,

$$\frac{\partial \sum_i \mathscr{E}_i^2(\hat{v}_c)}{\partial a_v} = 0, \frac{\partial \sum_i \mathscr{E}_i^2(\hat{v}_c)}{\partial b_v} = 0, \frac{\partial \sum_i \mathscr{E}_i^2(\hat{v}_c)}{\partial \alpha_v} = 0, \quad (31)$$

$$\frac{\partial \sum_i \mathscr{E}_i^2(\hat{v}_c)}{\partial \beta_v} = 0, \frac{\partial \sum_i \mathscr{E}_i^2(\hat{v}_c)}{\partial \chi_v} = 0, \quad (32)$$

equivalently we have,

$$\begin{aligned}
&\frac{\partial \sum_i \left(v_c(i) - \left(\frac{a_v}{1+\phi_i e^{-b_v \gamma_{dBi}}}\right)\right)^2}{\partial a_v} = 0,\\
&\frac{\partial \sum_i \left(v_c(i) - \left(\frac{a_v}{1+\phi_i e^{-b_v \gamma_{dBi}}}\right)\right)^2}{\partial b_v} = 0,\\
&\frac{\partial \sum_i \left(v_c(i) - \left(\frac{a_v}{1+\phi_i e^{-b_v \gamma_{dBi}}}\right)\right)^2}{\partial \alpha_v} = 0,\\
&\frac{\partial \sum_i \left(v_c(i) - \left(\frac{a_v}{1+\phi_i e^{-b_v \gamma_{dBi}}}\right)\right)^2}{\partial \beta_v} = 0,\\
&\frac{\partial \sum_i \left(v_c(i) - \left(\frac{a_v}{1+\phi_i e^{-b_v \gamma_{dBi}}}\right)\right)^2}{\partial \chi_v} = 0
\end{aligned} \quad (33)$$

Finally, by solving the system of equations in (33) according to the collected set of data, we have:

$$a_v = 1 - \frac{e}{3}, b_v = \frac{1}{4}, \alpha_v = -3, \beta_v = -2.5 \quad \text{and} \quad \chi_v = \frac{4}{3}$$

Therefore, after simplification (27) becomes as follows,

$$\begin{aligned}
\hat{v}_c &= \frac{1 - \frac{e}{3}}{1 + \exp\left[-2.5 \log_{10}(\gamma)\right] \left(\frac{4}{3} - \frac{3}{N^{2.5}}\right)} \\
&= \frac{1 - \frac{e}{3}}{1 + \gamma^{-1.08574} \left(\frac{4}{3} - \frac{3}{N^{2.5}}\right)}
\end{aligned} \quad (34)$$

5.2 Rate Outage Probability

Assuming that the achievable rate of the user of interest in three-cell OSGD system can be accurately approximated by log-normal distribution, i.e., $C \approx \mathscr{LN}(\hat{m}_c, \hat{v}_c)$ with mean m_c and variance v_c as expressed in (18) and (27) respectively. Then, the rate outage probability of this user for a certain target rate R can be computed from the cumulative distribution function, and it is expressed as follow:

$$\begin{aligned}
P_{outage}(R, \gamma, N) &= F_{C \sim \mathscr{LN}}(R | \hat{\mu}_c, \hat{\sigma}_c^2) \\
&= \int_0^R \frac{1}{c\sqrt{2\pi}\hat{\sigma}_c} e^{\frac{-(\ln(R) - \hat{\mu}_c)^2}{2\hat{\sigma}_c^2}} dc \\
&= \frac{1}{2}\left[1 + erf\left(\frac{(\ln(R) - \hat{\mu}_c)}{\hat{\sigma}_c\sqrt{2}}\right)\right] \\
&= \frac{1}{2} erfc\left(\frac{-(\ln(R) - \hat{\mu}_c)}{\hat{\sigma}_c\sqrt{2}}\right),
\end{aligned} \quad (35)$$

where, $\hat{\mu}_c$, $\hat{\sigma}_c^2$ are given by (15), (16) respectively, and the *erf* and *erfc* are the error function and the complementary error function respectively.

5.3 Effective Capacity of the Three-Cell OSGD System

In order to analyze the applicability of short packet communication to low latency, the effective capacity (EC) is used to find the maximum arrival rate for a given service rate, while satisfying the specific latency constraint [60]. On other words, EC can be used to find the maximum source rate (service rate) that the channel with the required delay constraint can handle [61].

Assuming a block fading scenario with frame duration T and buffering-queue decaying rate denoted by θ. Where the larger value of θ means more strict QoS conditions, while smaller values imply looser QoS guarantees. Specifically, when θ tends to zero, it implies delay-tolerant communication. On the other hand, when θ tends to infinity, it implies delay-limited communication. Then, the formula of the effective capacity (the maximum arrival rate) can be expressed as follows [62, 63],

$$C_e \triangleq \frac{-1}{T\theta} \log_e\left(\mathbb{E}\left\{e^{-T\theta C[n]}\right\}\right) \quad (36)$$

where $C[n]$ is the sample values of the instantaneous achievable rate.

Now, assuming the achievable rate of a system has log-normal distribution with mean $\hat{m}_c$ and variance $\hat{v}_c$, i.e.,

$$C \sim \mathscr{LN}(\hat{m}_c, \hat{v}_c), \quad (37)$$

and by defining the random variable S as follows,

$$S = e^{-\hat{\theta}C} \quad (38)$$

where, $\hat{\theta} = T\theta$.

Then, we can compute the effective capacity through the following steps: First, we should determine the expected

value of S, i.e.,

$$\begin{aligned}\Gamma &= \mathbb{E}\{S\} \\ &= \int_0^{\infty} e^{-\hat{\theta}c} \times \frac{1}{c\sigma_c\sqrt{2\pi}} e^{\frac{-(\ln c-\hat{\mu}_c)^2}{2\hat{\sigma}^2{}_c}} \\ &= \sum_{n=0}^{\infty} \frac{(-\hat{\theta})^n}{n!} e^{n\hat{\mu}+\frac{1}{2}n^2\hat{\theta}^2\hat{\sigma}^2{}_c}\end{aligned} \tag{39}$$

The expression in (39) can be seen as the Laplace transform of the log-normal distribution and it can be approximated as follows [64]

$$\begin{aligned}&\mathbb{E}\{C^l e^{-\hat{\theta}C}\} = \\ &\int_{-\infty}^{\infty} \frac{c^{l-1}}{\hat{\sigma}_c\sqrt{2\pi}} \times \exp\left\{-\hat{\theta}c - \frac{(\ln c-\hat{\mu}_c)^2}{2\hat{\sigma}^2{}_c}\right\} dc, \\ &= \frac{1}{\hat{\sigma}_c\sqrt{2\pi}} \times \int_{-\infty}^{\infty} \exp\left\{-\hat{\theta}e^u + lu - \frac{(u-\hat{\mu}_c)^2}{2\hat{\sigma}^2{}_c}\right\} du, \\ &\qquad\qquad l = 0,1,2,\cdots\end{aligned} \tag{40}$$

Second, we use the change of variables $u = \ln c$ to evaluate the above integral. Then, we approximate the exponent (the terms between the curly braces) with the second order of Taylor series expansion around the critical point ρ that maximize this exponent.

$$\begin{aligned}&\left\{\rho\, l - \frac{(\hat{\mu}_c-\rho)^2}{2\,\hat{\sigma}_c^2} - \hat{\theta}\,\mathrm{e}^{\rho} - (\rho-u)\left(l - \hat{\theta}\,\mathrm{e}^{\rho} + \frac{(\hat{\mu}_c-\rho)}{\hat{\sigma}_c^2}\right)\right. \\ &\qquad \left. - \left(\frac{\hat{\theta}\,\mathrm{e}^{\rho}}{2} + \frac{1}{2\,\hat{\sigma}_c^2}\right)(\rho-u)^2 + O\Big(-(\rho-u)^3\Big)\right\}\end{aligned} \tag{41}$$

For the case when $l = 0$, we can approximate the integral in (39) and obtain an accurate approximation for Γ as follows,

$$\begin{aligned}\widetilde{\Gamma} = \frac{1}{\hat{\sigma}_c\sqrt{2\pi}} \int_{-\infty}^{\infty} \exp\Bigg\{ &- \frac{(\hat{\mu}_c-\rho)^2}{2\,\hat{\sigma}_c^2} - \hat{\theta}\,\mathrm{e}^{\rho} \\ &- (\rho-u)\left(-\hat{\theta}\,\mathrm{e}^{\rho} + \frac{(\hat{\mu}_c-\rho)}{\hat{\sigma}_c^2}\right) \\ &- (\rho-u)^2\left(\frac{\hat{\theta}\,\mathrm{e}^{\rho}}{2} + \frac{1}{2\,\hat{\sigma}_c^2}\right)\Bigg\} du\end{aligned} \tag{42}$$

Eventually, selecting $\rho = -\mathrm{LW}\left(\hat{\theta}\hat{\sigma}_c^2 e^{\hat{\mu}_c} + \hat{\mu}_c\right)$ according to [64] will maximize the exponent in (41). Thus, the expression in (42) can be tightly transformed to,

$$\begin{aligned}\widetilde{\Gamma} = &\frac{1}{\sqrt{\mathrm{LW}(\hat{\theta}\hat{\sigma}^2{}_c e^{\hat{\mu}_c}) + 1}} \\ &\times \exp\left\{-\frac{\mathrm{LW}^2(\hat{\theta}\hat{\sigma}^2{}_c e^{\hat{\mu}_c}) + 2\,\mathrm{LW}(\hat{\theta}\hat{\sigma}^2{}_c e^{\hat{\mu}_c})}{2\hat{\sigma}^2{}_c}\right\},\end{aligned} \tag{43}$$

where, $\mathrm{LW}(\cdot)$ denotes the LambertW function, or the Omega function, $\mathrm{LW}(x)e^{\mathrm{LW}(x)} = x$ [65].
As a final step, we took the natural logarithm of $\widetilde{\Gamma}$ and normalize the result by $-\hat{\theta}$, thus, we have,

$$C_e = \frac{-1}{\hat{\theta}} \log_e(\widetilde{\Gamma}) \tag{44}$$

The final expression provides an approximation for the effective capacity of any system whose achievable rate distributed according to the log-normal probability density function. To compute the effective capacity of the massive MIMO three-cell OSGD system regarding to the normalized QoS exponent $\hat{\theta}$ and for SNR level γ, where the nodes are equipped with N antennas each, we can directly calculate $\hat{\mu}_c$ and $\hat{\sigma}_c$ from (15) and (16) with the use of (18) and (27), then, invoke those values into (43), and finally apply (44).

6 Results and Discussion

The main purpose of this section is to confirm the significant agreement between the obtained closed-form approximation formulas and the Monte-Carlo simulation results of the described system in Section 4. Hence, in this section we present the numerical results carried out by simulating a system of three interfering nodes deploying massive MIMO OSGD scheme. In all of the following scenarios, we assume strong interference environment, i.e., the α_i in (11) equals 1.

6.1 Validation of the Log-Normal Distribution Approximation

The accuracy of our proposal that log-normal distribution can be used to characterize the overall randomness of the achievable rate in case of using OSGD scheme is confirmed by the tight-fitting between the proposed and simulated probability density function (PDF) and cumulative distribution function (CDF) of the system achievable rate. This close match is valid for a wide range of the two factors of interest (γ and N). As shown in the figures (3, 4, 5, 6, 7 and 8) Monte-Carlo simulation results which plotted with the green stem-like shape, and the analytical results representing the log-normal curve shaped according the derived parameters ($\hat{m}_c$, $\hat{v}_c$) plotted with the continuous blue line, are in close fit for all scenarios. We have tested different number of antennas (10, 20 and 40) at different levels of SNR, starting from the power-limited regime with 0 dB SNR to the high SNR regime with 20 dB. This confirms the validity of our assumption and the derived formulas in (26) and (34). As expected the increase of the number of antennas or SNR level will increase the mean of the achievable rate as expressed in (26), which of course controls the shift of the histograms or the CDF plots to the right.

For deeper insight about the accuracy of the proposed approximation, we plotted the simulation results of the achievable rate versus the number of antennas ($1 \leq N \leq 40$) and the SNR in decibel ($-30\,dB \leq \gamma_{dB} \leq 60\,dB$), then, we interweaved this graph with a grid of generated points using the proposed approximation formulas in the same figure. The 3-D plots in Fig. 9 of the mean values of the achievable rate which are the resultant of simulation and the values computed via the approximation formula (26) show the match between both surfaces. We also evaluated the residuals between the two surfaces by computing the MSE between the simulation and the approximation points, and it is found to be less than 8×10^{-3}. This match is shown clearly once more in Fig. 10. From the findings in these two figures we again justify the accuracy of the obtained formula in (26).

Similarly, Fig. 11 shows the match between the mathematically approximation and the simulation-generated values for the achievable rate variance. In this case, computed MSE between the simulation and the analytical points is less than 5×10^{-7}. Our finding in this part clarify that the achievable rate variance is much affected by SNR γ than the number of antennas N. In particular it increases logarithmically with the SNR in the range of (-10 to 20) dB. The results shown in this figure again confirms validity of our derived formula to compute the achievable rate variance in (34).

6.2 Validation of the Outage Probability Formula

In this subsection, we aim to demonstrate the accuracy of the obtained formula the outage probability function (35). Therefore, we contrast the results attained through the Monte-Carlo simulation with graphs plotted using the proposed analytical formula in various scenarios. In the first case which presented in Fig. 12, we employed (16×16)-MIMO OSGD system with target rate of 32 bps/Hz, (32×32)-MIMO system with target rate of 64 bps/Hz, and (64×64)-MIMO system with target rate of 128 bps/Hz. In this scenario, we demanded a target rate that is a double of the employed antenna size.

From the results, one can notice that it seems for the system to maintain an outage probability lower than a specific level, it almost requires the same level of SNR for any antenna size. However, it is still true that the smaller systems are more efficient in utilizing the available SNR level. For instance, the systems with sizes of 16×16, 32×32 and 64×64 require (14.1, 14.2, and 14.4) decibels of SNR respectively to maintain the outage probability at 1%. The slight performance degradation in the larger systems is due to the residual of self-interference caused by the larger number of simultaneously transmitted streams.

In the second scenario, depicted in Fig. 13, we deployed (20×20, 30×30 and 40×40)-MIMO OSGD system to achieve target rates equal to the antenna size, i.e., (20, 30 and 40) bps/Hz respectively. In this case, we notice that we still need almost a fixed level of SNR to ensure the required outage probability. For example, the systems with sizes of 20×20, 30×30 and 40×40 require (4.55, 4.6, and 4.7) decibels of SNR respectively to retain the outage probability at 1%. Of course, the required SNR in this scenario is much lower than that for the first scenario, because we demand the target rate to be only 1 bps/Hz/antenna, while it was the double of that in the first scenario. It is worth mentioning here that doubling the required target rate per antenna does not require only doubling the power, which is a 3 dB increase in SNR, but it does require about a 9-10 dB increment. This is due to the nonlinear (logarithmic) relationship between the achievable rate and power.

All those scenarios revealed a good match between the system simulation results and the proposed mathematical approximation expression in (35).

6.3 Validation of the Effective Capacity Formula

In this subsection we used numerical results obtained from the simulation to validate the proposed closed-form expression of the effective capacity declared in (44) based on (43). Therefore, we ran Monte-Carlo setup to compute the effective capacity of the massive MIMO OSGD system, considering low and high SNR scenarios for different MIMO configuration sizes. The results of this subsection are shown in figures (14, 15, 16 and 17).

To obtain these results, we logarithmically increase $\hat{\theta}$ which represents multiplication of the frame duration T and the decaying rate of the buffering-queue θ. Here we should remind the reader that, for a fixed frame duration the larger value of $\hat{\theta}$ means more strict QoS conditions, hence a lower guaranteed bit rate can be transmitted. Clearly, the effective capacity degrades linearly with tightening up the QoS conditions. Also, it is obvious that the effective capacity is highly affected by the number of antennas and SNR of the system as shown in Fig. 18. It is similar to ergodic capacity increases linearly with the number of antennas, and logarithmally with the SNR level.

From all the presented results in this subsection, we can perceive the close match between the simulated and the analytical results for the effective capacity and that validates the derived mathematical approximation in (43 and 44).

7 Conclusion

In this paper we derived a simple closed-form approximation for the desired user achievable rate and effective capacity in the massive MIMO system occupied with few clients utilizing the successive group decoders to mitigate interference. Also, we developed a tight mathematical approx-

imation expression for the outage probability of this system. Through the outcomes of this work, it is established that for the large-enough system, the mean of the achievable rate or ergodic capacity increases linearly with the rise in the number of antennas N, and logarithmically with SNR γ. In addition, we noticed that the variance of this achievable rate is increasing with SNR. On the other hand, this variance is decreasing with the increase of antenna array size N. Also, we noticed that the effective capacity of the considered system linearly decreases with the increase of the multiplication of the frame duration and the decaying rate of the buffering-queue. Furthermore, it is observed that to maintain the outage probability of the investigated system at a specific level, with target rate proportional to the antenna size, the required SNR will be almost the same regardless the number employed antennas. However, it is still true that the smaller systems are slightly efficient in utilizing the available SNR level. Finally, we say that we plan to deploy the methodology presented in this paper for future work to explore the effect of other performance-limiting parameters of the wireless systems, which we did not consider in this research. For instance: imperfect channel estimation, spatial channels correlation, unequal power allocation and the number of interfering nodes to investigate their impact on the overall performance of the considered systems, with an emphasis on those systems which employ receive-side interference cancellation techniques.

Acknowledgments

The authors express their gratitude to Chinonso Ezeobi, a distinguished engineer at Huawei Technologies Nigeria, for reviewing the language of this paper, and for his valuable remarks.

Compliance with ethical standards

Conflict of interest On behalf of all authors, the corresponding author states that there is no conflict of interest.

Figures

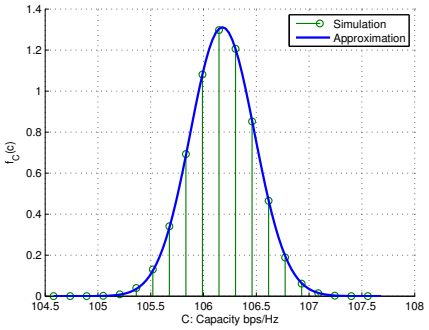

Fig. 3 Pdf of achievable rate for $N = 40$ and $SNR = 20$ dB.

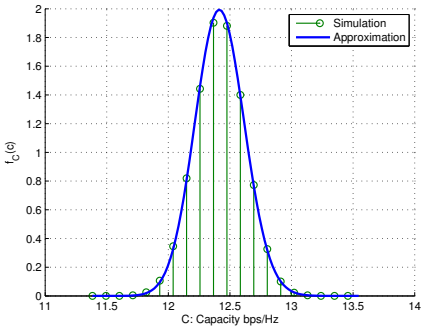

Fig. 4 Pdf of achievable rate for $N = 20$ and $SNR = 0$ dB.

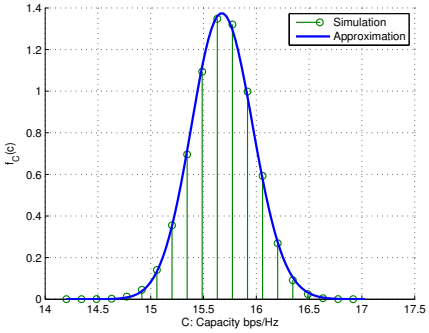

Fig. 5 Pdf of achievable rate for $N = 10$ and $SNR = 10$ dB.

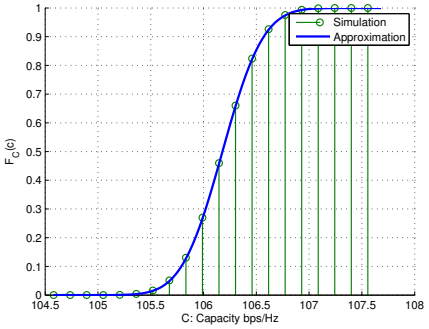

Fig. 6 CDF of achievable rate for $N = 40$ and $SNR = 20$ dB.

References

1. Wang, C.-X., Haider, F., Gao, X., You, X.-H., Yang, Y., Yuan, D., Aggoune, H.M., Haas, H., Fletcher, S., Hepsaydir, E.: Cellular architecture and key technologies for 5g wireless communication networks. IEEE communications magazine **52**(2), 122–130 (2014)
2. Zhang, R., Hanzo, L.: Wireless cellular networks. Vehicular Technology Magazine, IEEE **5**(4), 31–39 (2010). doi:10.1109/MVT.2010.939106

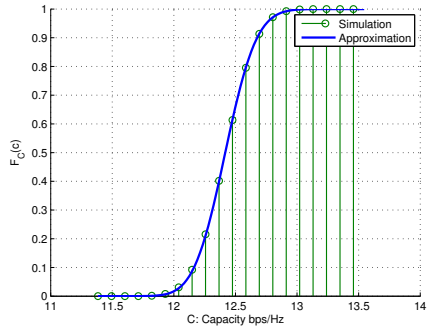

Fig. 7 CDF of achievable rate for $N = 20$ and $SNR = 0$ dB.

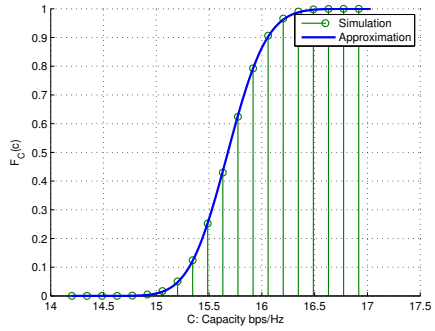

Fig. 8 CDF of achievable rate for $N = 10$ and $SNR = 10$ dB.

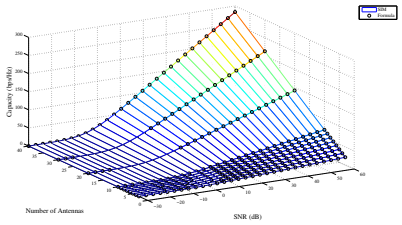

Fig. 9 Achievable rate mean versus SNR(dB) and the number of antennas.

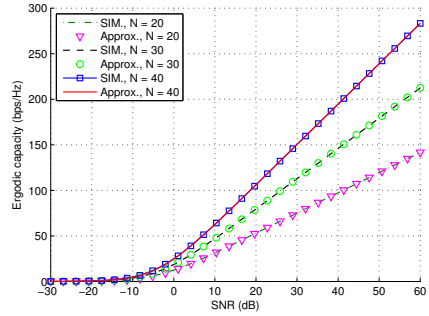

Fig. 10 Ergodic capacity versus SNR(dB) for different number of antennas.

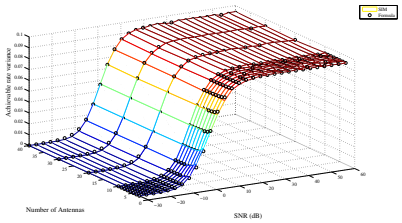

Fig. 11 Achievable rate variance versus SNR(dB) and the number of antennas.

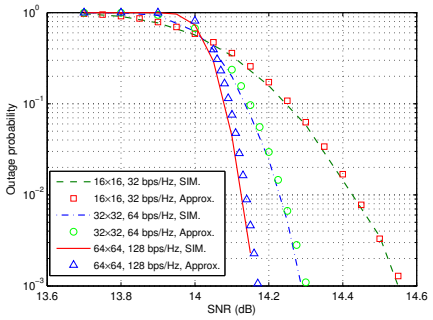

Fig. 12 Outage probability of the $(16 \times 16,\ 32 \times 32$ and $64 \times 64)$-MIMO OSGD system.

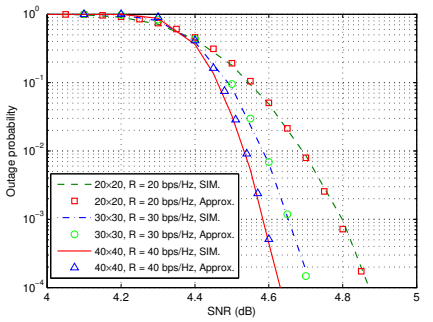

Fig. 13 Outage probability of the $(20 \times 20,\ 30 \times 30$ and $40 \times 40)$-MIMO OSGD system.

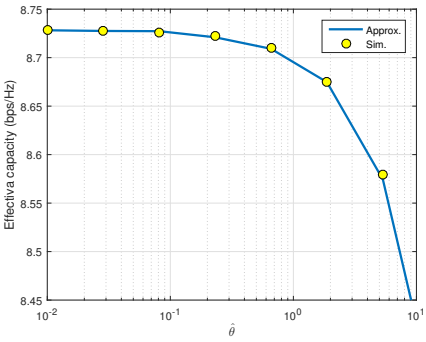

Fig. 14 Effective capacity versus $\hat{\theta}$, of OSGD system with $N = 10$ and $SNR = 3$ dB.

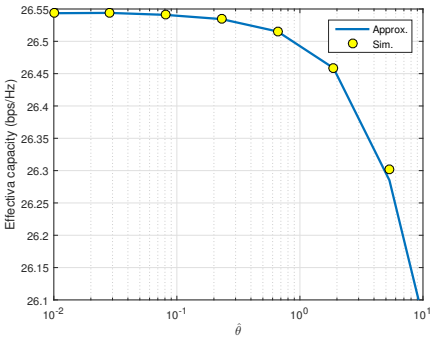

Fig. 15 Effective capacity versus $\hat{\theta}$, of OSGD system with $N = 10$ and $SNR = 20$ dB.

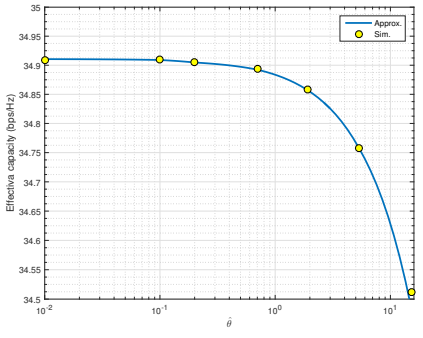

Fig. 16 Effective capacity versus $\hat{\theta}$, of OSGD system with $N = 40$ and $SNR = 3$ dB.

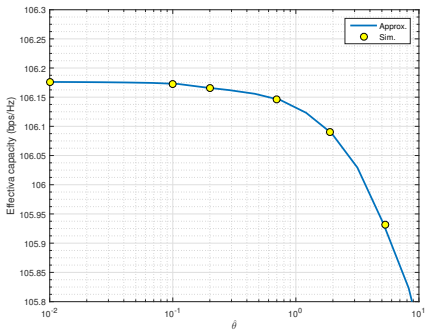

Fig. 17 Effective capacity versus $\hat{\theta}$, of OSGD system with $N = 40$ and $SNR = 20$ dB.

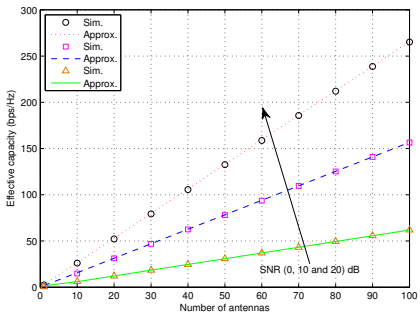

Fig. 18 Effective capacity versus N, for OSGD system with ($SNR = 0, 10$ and 20) dB and $\hat{\theta} = 10$.

3. Cho, H.-N., Lee, J.-W., Lee, Y.-H.: Coordinated transmission of interference mitigation and power allocation in two-user two-hop mimo relay systems. EURASIP Journal on Wireless Communications and Networking **2010**(1), 132910 (2010). doi:10.1155/2010/132910
4. Lee, H., Oh, D., Lee, Y.: Coordinated user scheduling with transmit beamforming in the presence of inter-femtocell interference. In: 2011 IEEE International Conference on Communications (ICC), pp. 1–5 (2011). doi:10.1109/icc.2011.5963055
5. Dowhuszko, A.A., Hämäläinen, J., Elsherif, A.R., Ding, Z.: Performance of transmit beamforming for interference mitigation with random codebooks. In: 8th International Conference on Cognitive Radio Oriented Wireless Networks, pp. 190–195 (2013). doi:10.1109/CROWNCom.2013.6636816
6. Chen, Z., Li, H., Cui, G., Rangaswamy, M.: Adaptive transmit and receive beamforming for interference mitigation. IEEE Signal Processing Letters **21**(2), 235–239 (2014). doi:10.1109/LSP.2014.2298497
7. Eliardsson, P., Wiklundh, K., Axell, E., Stenumgaard, P.: Mitigation of co-channel interference by transmit power control. In: 2015 IEEE International Symposium on Electromagnetic Compatibility (EMC), pp. 189–193 (2015). doi:10.1109/ISEMC.2015.7256156
8. Ardalani, N., Mirmohseni, M., Aref, M.R.: Three-user interference channel with common information: a rate splitting-based achievability scheme. Communications, IET **8**(4), 462–470 (2014). doi:10.1049/iet-com.2013.0567
9. Hou, R., Xie, Y., Lui, K., Li, J.: Scheduling in dense small cells with successive interference cancellation. Communications Letters, IEEE **PP**(99), 1–1 (2014). doi:10.1109/LCOMM.2014.2318310
10. Toboso, A.U., Loyka, S., Gagnon, F.: Optimal detection ordering for coded v-blast. Communications, IEEE Transactions on **62**(1), 100–111 (2014). doi:10.1109/TCOMM.2013.121413.130268
11. Blough, D.M., Santi, P., Srinivasan, R.: On the feasibility of unilateral interference cancellation in mimo networks. Networking, IEEE/ACM Transactions on **PP**(99), 1–1 (2014). doi:10.1109/TNET.2013.2286829
12. Prasad, N., Wang, X.: Outage minimization and rate allocation for the multiuser gaussian interference channels with successive group decoding. Information Theory, IEEE Transactions on **55**(12), 5540–5557 (2009). doi:10.1109/TIT.2009.2032725
13. Gong, C., Abu-Ella, O., Wang, X., Tajer, A.: Constrained group decoder for interference channels. JOURNAL Of COMMUNICATIONS **7**(5), 382–390 (2012)
14. Telatar, I.E.: Capacity of multi-antenna gaussian channels. EUROPEAN TRANSACTIONS ON TELECOMMUNICATIONS **10**, 585–595 (1999)
15. Rapajic, P.B., Popescu, D.: Information capacity of a random signature multiple-input multiple-output channel. IEEE Transactions on Communications **48**(8), 1245–1248 (2000). doi:10.1109/26.864159
16. Kamath, M.A., Hughes, B.L.: The asymptotic capacity of multiple-antenna rayleigh-fading channels. IEEE Transactions on Information Theory **51**(12), 4325–4333 (2005). doi:10.1109/TIT.2005.858966
17. Artigue, C., Loubaton, P.: On the precoder design of flat fading mimo systems equipped with mmse receivers: A large-system approach. IEEE Transactions on Information Theory **57**(7), 4138–4155 (2011). doi:10.1109/TIT.2011.2145710
18. Tran, T.X., Teh, K.C.: Performance analysis of massive multiuser multiple-input multiple-output systems with block diagonalisation. IET Communications **10**(7), 832–838 (2016). doi:10.1049/iet-com.2015.0400
19. Shen, J., Zhang, J., Letaief, K.B.: Downlink user capacity of massive mimo under pilot contamination. IEEE Transactions on Wireless Communications **14**(6), 3183–3193 (2015). doi:10.1109/TWC.2015.2403317

20. Anokye, P., Ahiadormey, R.K., Song, C., Lee, K.: Achievable sum-rate analysis of massive mimo full-duplex wireless backhaul links in heterogeneous cellular networks. IEEE Access **6**, 23456–23469 (2018). doi:10.1109/ACCESS.2018.2828598
21. Weber, S.P., Andrews, J.G., Yang, X., de Veciana, G.: Transmission capacity of wireless <emphasis>ad hoc</emphasis> networks with successive interference cancellation. IEEE Transactions on Information Theory **53**(8), 2799–2814 (2007). doi:10.1109/TIT.2007.901153
22. Sheng, M., Liu, J., Wang, X., Zhang, Y., Sun, H., Li, J.: On transmission capacity region of d2d integrated cellular networks with interference management. IEEE Transactions on Communications **63**(4), 1383–1399 (2015)
23. Chandrasekhar, R., Navya, R., Kumari, P.K., Kausal, K., Bharathi, V., Singh, P.: Performance evaluation of mimo-noma for the next generation wireless communications. In: 2021 3rd International Conference on Signal Processing and Communication (ICPSC), pp. 631–636 (2021). IEEE
24. Haider, M., Bal, A., Sur, M., Chowdhury, N., Chowdhury, A.: Analyzing hybrid noma schemes underlining energy-spectral efficiency and sic tradeoff. In: 2021 13th International Conference on Communication Software and Networks (ICCSN), pp. 377–382 (2021). IEEE
25. Shuai, H., Guo, K., An, K., Zhu, S.: Noma-based integrated satellite terrestrial networks with relay selection and imperfect sic. IEEE Access **9**, 111346–111357 (2021). doi:10.1109/ACCESS.2021.3103944
26. Haghi, A., Khandani, A.K.: Rate splitting and successive decoding for gaussian interference channels. IEEE Transactions on Information Theory **67**(3), 1699–1731 (2021)
27. Suard, B., Xu, G., Liu, H., Kailath, T.: Uplink channel capacity of space-division-multiple-access schemes. IEEE Transactions on Information Theory **44**(4), 1468–1476 (1998)
28. Christopoulos, D., Chatzinotas, S., Matthaiou, M., Ottersten, B.: Capacity analysis of multibeam joint decoding over composite satellite channels. In: 2011 Conference Record of the Forty Fifth Asilomar Conference on Signals, Systems and Computers (ASILOMAR), pp. 1795–1799 (2011). doi:10.1109/ACSSC.2011.6190331
29. Bresler, G., Parekh, A., David, N.: The approximate capacity of the many-to-one and one-to-many gaussian interference channels. IEEE Transactions on Information Theory **56**(9), 4566–4592 (2010)
30. Shlezinger, N., Eldar, Y.C.: Spectral efficiency of noncooperative uplink massive mimo systems with joint decoding. In: ICASSP 2019-2019 IEEE International Conference on Acoustics, Speech and Signal Processing (ICASSP), pp. 4779–4783 (2019). IEEE
31. Abu-Ella, O., Elmusrati, M.: Capacity approximation of massive mimo with optimal successive group decoding system. In: 2014 Eighth International Conference on Next Generation Mobile Apps, Services and Technologies, pp. 254–259 (2014). doi:10.1109/NGMAST.2014.13
32. Abu-Ella, O., Wang, X.: Large-scale multiple-input-multiple-output transceiver system. Communications, IET **7**(5), 471–479 (2013). doi:10.1049/iet-com.2012.0471
33. Liu, Y., Qin, Z., Elkashlan, M., Gao, Y., Nallanathan, A.: Non-orthogonal multiple access in massive mimo aided heterogeneous networks. In: 2016 IEEE Global Communications Conference (GLOBECOM), pp. 1–6 (2016). IEEE
34. Dai, L., Wang, B., Ding, Z., Wang, Z., Chen, S., Hanzo, L.: A survey of non-orthogonal multiple access for 5g. IEEE Communications Surveys Tutorials **20**(3), 2294–2323 (2018). doi:10.1109/COMST.2018.2835558
35. Hur, S., Kim, T., Love, D.J., Krogmeier, J.V., Thomas, T.A., Ghosh, A.: Millimeter wave beamforming for wireless backhaul and access in small cell networks. IEEE Transactions on Communications **61**(10), 4391–4403 (2013). doi:10.1109/TCOMM.2013.090513.120848
36. Andrews, J.G., Buzzi, S., Choi, W., Hanly, S.V., Lozano, A., Soong, A.C.K., Zhang, J.C.: What will 5g be? IEEE Journal on Selected Areas in Communications **32**(6), 1065–1082 (2014). doi:10.1109/JSAC.2014.2328098
37. Muirhead, D., Imran, M.A., Arshad, K.: A survey of the challenges, opportunities and use of multiple antennas in current and future 5g small cell base stations. IEEE Access **4**, 2952–2964 (2016). doi:10.1109/ACCESS.2016.2569483
38. De Ree, M., Mantas, G., Radwan, A., Mumtaz, S., Rodriguez, J., Otung, I.E.: Key management for beyond 5g mobile small cells: A survey. IEEE Access **7**, 59200–59236 (2019). doi:10.1109/ACCESS.2019.2914359
39. Usman, M., Wajid, M., Ansari, M.D.: Enabling Technologies for Next Generation Wireless Communications, (2020)
40. Gong, C., Tajer, A., Wang, X.: Interference channel with constrained partial group decoding. Communications, IEEE Transactions on **59**(11), 3059–3071 (2011). doi:10.1109/TCOMM.2011.082111.100624
41. Zheng, K., Zhao, L., Mei, J., Shao, B., Xiang, W., Hanzo, L.: Survey of large-scale mimo systems. IEEE Communications Surveys Tutorials **17**(3), 1738–1760 (2015). doi:10.1109/COMST.2015.2425294
42. Hansryd, J., Edstam, J., Olsson, B.-E., Larsson, C.: Non-line-of-sight microwave backhaul for small cells. Ericsson Review, 1–8 (2013)
43. Tabassum, H., Sakr, A.H., Hossain, E.: Analysis of massive mimo-enabled downlink wireless backhauling for full-duplex small cells. IEEE Transactions on Communications **64**(6), 2354–2369 (2016). doi:10.1109/TCOMM.2016.2555908
44. Claussen, H., Lopez-Perez, D., Ho, L., Razavi, R., Kucera, S.: Backhaul for Small Cells. IEEE, ??? (2018). doi:10.1002/9781119307600.ch14. https://ieeexplore.ieee.org/document/8233743
45. Huq, K.M.S., Rodriguez, J.: Backhauling 5G Small Cells with Massive-MIMO-Enabled mmWave Communication, pp. 29–53. Wiley, ??? (2016). doi:10.1002/9781119170402.ch3
46. Bjornson, E., Van der Perre, L., Buzzi, S., G. Larsson, E.: Massive mimo in sub-6 ghz and mmwave: Physical, practical, and use-case differences. IEEE Wireless Communications, 2–10 (2019). doi:10.1109/MWC.2018.1800140
47. Giordani, M., Polese, M., Mezzavilla, M., Rangan, S., Zorzi, M.: Toward 6g networks: Use cases and technologies. IEEE Communications Magazine **58**(3), 55–61 (2020)
48. Hong, W., Jiang, Z.H., Yu, C., Hou, D., Wang, H., Guo, C., Hu, Y., Kuai, L., Yu, Y., Jiang, Z., Chen, Z., Chen, J., Yu, Z., Zhai, J., Zhang, N., Tian, L., Wu, F., Yang, G., Hao, Z.-C., Zhou, J.Y.: The role of millimeter-wave technologies in 5g/6g wireless communications. IEEE Journal of Microwaves **1**(1), 101–122 (2021). doi:10.1109/JMW.2020.3035541
49. Xi, J., Zhang, J., Tian, L., Wu, Y.: Capacity analysis based on channel measurements of massive mu-mimo system at 3.5 ghz. In: 2017 3rd IEEE International Conference on Computer and Communications (ICCC), pp. 79–83 (2017). doi:10.1109/CompComm.2017.8322518
50. Zheng, K., Ou, S., Yin, X.: Massive mimo channel models: A survey. International Journal of Antennas and Propagation (2014)
51. Goldsmith, A.J., Varaiya, P.P.: Capacity of fading channels with channel side information. IEEE Transactions on Information Theory **43**(6), 1986–1992 (1997). doi:10.1109/18.641562
52. Abdi, A., Barger, H.A., Kaveh, M.: A simple alternative to the lognormal model of shadow fading in terrestrial and satellite channels. In: IEEE 54th Vehicular Technology Conference. VTC Fall 2001. Proceedings (Cat. No.01CH37211), vol. 4, pp. 2058–20624 (2001). doi:10.1109/VTC.2001.957106

53. Cotton, S.L., Scanlon, W.G.: Higher order statistics for lognormal small-scale fading in mobile radio channels. IEEE Antennas and Wireless Propagation Letters **6**, 540–543 (2007). doi:10.1109/LAWP.2007.909968
54. Kaur, A., Malhotra, J.: Cascade fading channel models for wireless communication-a survey. In: International Journal of Computer Applications, vol. 89, pp. 22–25 (2014)
55. Shankar, P.M.: Fading and Shadowing in Wireless Systems, 2nd edn. Springer, ??? (2017)
56. Karagiannis, G.A., Panagopoulos, A.D.: Dynamic lognormal shadowing framework for the performance evaluation of next generation cellular systems. Future Internet **11**(5) (2019). doi:10.3390/fi11050106
57. Laourine, A., Stephenne, A., Affes, S.: On the capacity of log-normal fading channels. IEEE Transactions on Communications **57**(6), 1603–1607 (2009). doi:10.1109/TCOMM.2009.06.070109
58. Heliot, F., Chu, X., Hoshyar, R., Tafazolli, R.: A tight closed-form approximation of the log-normal fading channel capacity. IEEE Transactions on Wireless Communications **8**(6), 2842–2847 (2009). doi:10.1109/TWC.2009.080972
59. Deping, L.: Some properties of lognormal distributions and its modification. The International Nuclear Information System (INIS) **26**(22), 57–69 (1993)
60. Amjad, M., Musavian, L., Aïssa, S.: Effective Capacity of NOMA with Finite Blocklength for Low-Latency Communications (2020). 2002.07098
61. Amjad, M., Musavian, L., Rehmani, M.H.: Effective capacity in wireless networks: A comprehensive survey. IEEE Communications Surveys & Tutorials **21**(4), 3007–3038 (2019)
62. Gursoy, M.C.: MIMO wireless communications under statistical queueing constraints. Information Theory, IEEE Transactions on **57**(9), 5897–5917 (2011). doi:10.1109/TIT.2011.2162168
63. Aman, W., Rahman, M.M.U., Ansari, S., Nasir, A.A., Qaraqe, K., Imran, M.A., Abbasi, Q.H.: On the effective capacity of irs-assisted wireless communication. Physical Communication **47**, 101339 (2021)
64. Nandayapa, L.R., Asmussen, S., Jensen, J.L.: Approximations of the laplace transform of a lognormal random variable. In: Conference in Honour of Søren Asmussen: New Frontiers in Applied Probability, School of Mathematics and Physics, The University of Queensland, Denmark. (2011)
65. Corless, R.M., Gonnet, G.H., Hare, D.E.G., Jeffrey, D.J., Knuth, D.E.: On the Lambert W function. Adv. Comput. Math **5**, 329 (1996)